Molecular dynamics simulations of ion transport through carbon nanotubes. III. Influence of the nanotube radius, solute concentration, and applied electric fields on the transport properties

Titus A. Beu[a)]
Faculty of Physics, University "Babeş -Bolyai," 400084 Cluj-Napoca, Romania

(Received 17 February 2011; accepted 6 July 2011; published online 29 July 2011)

The present investigations continue previous research on transport in aqueous ionic solutions through carbon nanotubes. Specifically, the effects of the nanotube radius, solute concentration, and applied external electric fields on the transport properties are investigated in terms of mobilities, currents, and pairing times of the solute ions. The simulated transport features are corroborated with general theoretical results of nanofluidics (such as the linear log-log regime of the nanochannel conductance as function of the solute concentration and the current-voltage curve of the channel). Discontinuities in the partial ionic currents are explained on the basis of a recent theoretical model of quantized ionic conductance in nanopores, developed by Zwolak *et al*. Correlations between the structural and dynamic properties are established, linking causally the highly structured spatial density profiles, the ion pairing phenomenon and the ionic currents. © *2011 American Institute of Physics*. [doi:10.1063/1.3615728]

I. INTRODUCTION

The present paper is the third in a series devoted to the systematic study by atomistic molecular dynamics (MD) simulations of the ion transport through "armchair"-type (n, n) carbon nanotubes (CNTs) of chiralities ranging from (8,8) to (12,12) filled with NaCl and NaI solutions.

Our previous papers[1,2] (referred to in the following as Papers I and II) have demonstrated that the detailed molecular structure of the solution inside the nanopore is crucial to understanding the ion permeation process and the general findings are consistent with those from the literature.[3–9] Nevertheless, the present series of simulations extends the scope of the so far available theoretical description of the permeation through CNTs and provides new insights by the ranges of considered CNT radii, solute concentrations, and applied electric fields, and, not in the least, by the achieved accuracy.

In Paper I, the dependences of diverse transport features on the solute specificity, the nanotube geometry, and the various atomic models employed have been addressed and interpreted in interrelation with the solution structuring and the energy barriers faced by the solute components. In particular, the detailed analysis of the relevance of molecular and ionic polarizability has revealed that, despite the local enhancement of the density profiles, the density peak positions and, moreover, the ionic currents are practically insensitive to the consideration of polarizability.

In Paper II, the solutions have been shown to maintain an invariant structuring (density peak pattern) at the carbon walls, irrespective of solute concentration, and applied axial electric field. Water forms well-defined boundary layers with the hydrogens located preferentially on the inner side, where they optimally hydrate the anions. The effect of the increase of ion concentration and/or axially applied electric field is to enhance the magnitudes of the density peaks, but not to change their positions. The significant increase of the coordinations of the solution components as functions of the pore radius confirms the frustrated neighborhood in the narrow nanochannels, but the bulk situation is reached rather soon (for O–O already in the CNT (10,10)).

The longitudinal channel voltage, caused jointly by the axial electric field and the electrochemical double layer formed at the membrane walls, can be described to a good approximation by an anion-specific *power-law* dependence on the average solute concentration and, respectively, by a *linear* dependence on the applied axial electric field (which appears to be anion non-specific). Another noteworthy result is the Donnan-type[10–12] *logarithmic* dependence of the channel voltage on the axial density maximum of the solute ions.

The present work focuses specifically on the effects of the solute concentration and applied external electric fields on the transport properties of CNTs. The transport of the solution components through the CNTs is characterized by means of dynamic properties, such as diffusion coefficients, ion currents, drift mobilities, and ion pairing times, which are analyzed with emphasis on their interrelation and causal link. In addition, certain dependences on the CNT radius (as, for instance, pair distribution functions, coordinations, and ion pairing) are also presented, complementing the information reported previously. The simulated properties are based on averages over the largest data collection times reported in the literature (0.8 μs), providing accurate estimates of the measured quantities.

II. SIMULATION DETAILS

The simulations from which the present results stem have been performed by a homemade computer code (MD-squad), relying on a MD methodology which was presented

a)Electronic mail: titus.beu@phys.ubbcluj.ro.

extensively in Papers I and II. Among the distinctive features, worth mentioning are the rigid-body dynamics in the quaternion representation[13] used for the water molecules and the P^3M mesh-based FFT-accelerated Ewald sum method[14,15] employed for handling the complex electrostatics in the presence of periodic boundary conditions. The molecular representation used for water has been the non-polarizable four-site model TIP4P of Jorgensen and co-workers[16,17] and, as representative halides from the Hofmeister series, we have selected chloride and iodide.

The channel model consists of a rigid non-polar "armchair"-type (n, n) CNT of length 60.17 Å enclosed symmetrically by two neutral graphene planes and two reservoirs.[1,2] The simulation cell has been adjusted in all cases such as to produce for 1000 water molecules a density of 1 g/cm^3 relative to the accessible volume. Ion concentrations from ~0.28 M to 1.66 M have been considered, resulting from 10, 20, 30, 40, 50, and, respectively, 60 ions of both species. The ions have been driven through the nanochannel by homogeneous electric fields of 0.005, 0.01, 0.02, 0.03, 0.04, and 0.05 V/Å, applied parallel to the channel axis.

For each particular solute type, nanotube radius, ion concentration, and applied electric field, a total evolution time of 0.8 μs was simulated with a time step of 2.5 fs at constant temperature ($T = 300$ K). The preparation of the initial configurations has been accomplished starting with an originally empty channel and densely filled reservoirs, allowing the solution to relax into the channel and finally equilibrating the system for 1 ns. Upper bounds for the inaccuracies of the measured quantities have been obtained as differences with respect to the equivalent results obtained from independent trajectory ensembles encompassing the half data collection time (0.4 μs).

III. RESULTS AND DISCUSSION

A. Diffusion coefficients

The mobility of the solute ions inside the CNTs is affected by significant fluctuations due to the relatively small number of transiting ions and, more generally, due to the fact that the system is highly inhomogeneous and out of equilibrium. Hence, describing the transport of the solution components requires special numerical techniques to compensate for the poor statistics inside the nanopore, both for low solute concentrations and low applied axial electric fields.

Even though the applicability of classical diffusion coefficients might seem questionable, in several recent works regarding the ionic transport through nanopores under the influence of explicit axial voltages (for example, Refs. 5 and 18) variants of Einstein's formula, based on the time averaged variance of the axial position, have been employed. We have chosen to implement instead the perfectly equivalent Green-Kubo formula, which involves the time integrated velocity autocorrelation function[13]

$$D = \lim_{\tau\to\infty} \frac{1}{3} \int_0^\tau \langle \mathbf{v}(0) \cdot \mathbf{v}(t) \rangle \, dt. \qquad (1)$$

The practical reason for preferring this definition is that, in conjunction with periodic boundary conditions, Einstein's formula requires double book-keeping of (periodicity-corrected/uncorrected) particle positions.

With a view to improving the quality of the measured diffusion coefficients, besides averaging over large ensembles of trajectories, we have also devised a technique for independently and dynamically choosing the optimal velocity sampling intervals for each solution component, by resetting the time origin whenever, due to velocity decorrelation, the relative contributions to the autocorrelation functions become irrelevant.

The *non-directional* diffusion coefficients calculated from Eq. (1) are dominated in the absence of applied voltages by the diffusion perpendicular to the CNT and, with increasing axial electric field strengths, by axial dispersion. For a particle species carrying charge q, these effective diffusion coefficients can be related to the diffusive mobility by Einstein's relation, $\mu_D = qD/k_\mathrm{B}T$.

The basic definitions of both the diffusion coefficient and the associated mobility pertain actually to homogeneous systems under equilibrium conditions. It is important, thus, to bear in mind the conceptual differences between the unbiased Brownian-motion-based coefficients and the biased effective diffusion coefficients discussed here. The derived diffusive mobility, μ_D, accounts obviously also for the diffusion perpendicular to the CNT and cannot be identified directly with the actual electrophoretic (drift) mobility, $\mu_E = v_z/E_z$ (with E_z the axial electric field strength and v_z the electrophoretic drift velocity), which will be discussed in Sec. III B. As will be pointed out below, the dependences of the effective diffusion coefficients inside the CNTs on the applied voltage are rather useful to extrapolate the zero-field coefficients of the radial diffusion, which, for the same solute concentration, are incomparably more difficult to obtain from equilibrium simulations.

The diffusion coefficients we have obtained for the water molecules and solute ions can be seen in Fig. 1 to decrease monotonically with increasing total number of solute ions. The dependences are discretely nonlinear, with a more abrupt initial decay, anticipating an asymptotic lower bound. It is noteworthy that the values for the solute ions corresponding to the lowest solute concentration, apparently departing from the general trend and suggesting statistical fluctuations, are actually in line with both the experimental and calculated self-diffusion coefficients in electrolyte solutions reported by Turq and co-workers.[19,20] In fact, the values reported for Cl^- (Fig. 1 of Ref. 19), corresponding to bulk rather than confined solutions, vary less than those reported here, dropping in the considered interval of solute concentrations by only 5% to about 0.19 Å^2/ps, but show the same more pronounced initial decrease for low concentrations. As for the cations, the mobilities reported in Ref. 20 for Na^+ are again consistent with the present ones.

The reduced diffusion in the pores as compared to the bulk reflects, on one hand the constrained average flow along cylindrical flux layers and on the other hand by virtue of the quite close values of the coefficients for water and ions, the fact that the ions travel partially surrounded by their solvation shells. The latter finding is supported also by the water flux accompanying each exiting ion, aspect which is

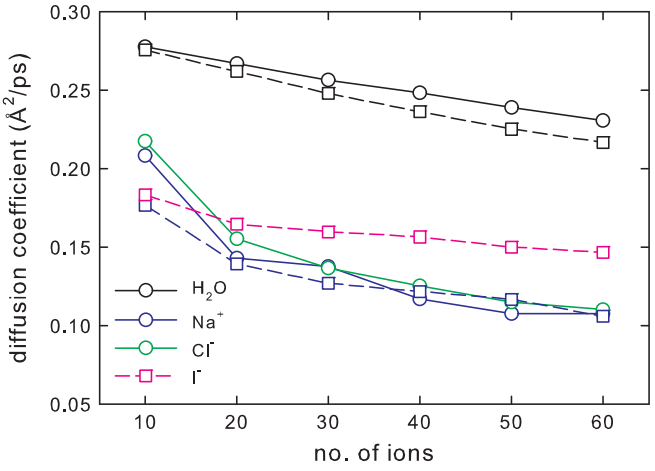

FIG. 1. Diffusion coefficients for water and ions in the CNT (10,10) subject to an axial electric field of 0.02 V/Å as functions of the solute ion concentration. Continuous (dashed) lines correspond to the NaCl (NaI) solution.

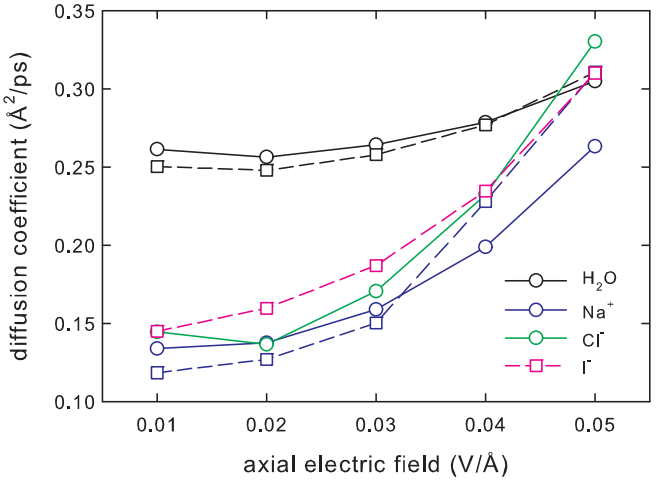

FIG. 2. Diffusion coefficients for water and ions in the CNT (10,10) for NaCl and NaI solutions composed of 30 solute ions as functions of the axial electrostatic field. Continuous (dashed) lines correspond to the NaCl (NaI) solution.

addressed in Sec. III B. The larger diffusion coefficient of I^- as compared to Cl^- (seen in Fig. 1) is perfectly consistent with the ionic currents discussed in the following and is a direct consequence of the larger average radius of the flux tubes for the I^- ions (as shown by the radial density profiles plotted in Fig. 1 of Paper II).

It is worth noting the agreement of the diffusion coefficient reported by Peter and Hummer[5] for the CNT (10,10) (0.23 ± 0.02 Å^2/ps) with the values 0.21 and 0.22 Å^2/ps, we have found for Na^+ and Cl^- in our lowest concentration solution (made up of 5 anion-cation pairs).

Contrary to the declining dependence of the diffusion coefficients on the solute concentration, the axial electric field enhances, as expected, the effective diffusivity of all solution components (Fig. 2). While for water the moderate increase is an indirect effect of the formation of solvation shells around the transiting solute ions, the increase for the latter ones is particularly pronounced. To a good approximation, the values for the Na^+ and I^- ions can be fitted with exponentials, reflecting that the electric field reduces their activation energy for the biased diffusion process through the CNTs. A similar enhancement of the self-diffusion inside the pore with the strength of the electric field was reported by Dzubiella and co-workers[3,4] and it can be correlated with the change of the water structuring inside the pore in the presence of high electric fields, concretely, with the disruption of the tetrahedral hydrogen bond network which water forms otherwise under equilibrium conditions.

Even more informative than the actual dependences of the effective diffusivities on the applied voltage is the possibility to extrapolate their zero-field limits, which are obviously dominated by the equilibrium diffusion perpendicular to the CNT axis. Moreover, under zero-field conditions, both the formula for the diffusion coefficient Eq. (1) and Einstein's relation for the mobilities, reflecting electrophoretic equilibrium, become rigorous. The values are situated around 0.25 Å^2/ ps for the water molecules and between 0.12 and 0.15 Å^2/ps for the solute ions, with the corresponding mobilities inside the CNT ranging for the considered temperature ($T = 300$ K) from 4.6 Å^2/V ps for Na^+ to 5.6 Å^2/V ps for I^-. Obtaining these values from static pore-filling simulations is cumbersome and, due to the inevitably poorer sampling caused by the trapping of the system within accumulation basins in the phase space, much larger trajectory ensembles than the ones employed in the present dynamic simulations are necessary to reach comparable accuracy.

In Sec. III B, the diffusional mobilities are compared with the drift mobilities derived from the average passage times of the ions through the nanotube.

B. Ionic currents

Some of the most descriptive transport features produced in the present simulations are the ionic currents. Considering opposite reference directions for the anion and cation fluxes, the ionic current is defined simply as the net average number of ions transiting the pore per nanosecond. In order to discern the contributions of the different ion species, besides the net total currents, the passage rates due to the Na^+ cations solely have been analyzed as well.

In Paper I, the ion currents have been shown to have a strong dependence on the pore radius and an anion-specific behavior materialized in ionic currents for the NaI solution with up 30% larger than for the NaCl solution. The (8,8) CNT appears to be very little permeable to ions, enabling under all conditions low currents of about 0.05 nA, which are in line with the results of Dzubiella and co-workers,[3,4] Peter and Hummer,[5] and Corry,[6] evidencing the impermeability for chiralities lower than (7,7).

For the sake of the following discussion, which will concentrate on the effect of the quantized ionic conductance in nanopores, recently described theoretically by Zwolak and co-workers,[8,9] the net ionic currents for the NaI solution, along with the partial Na^+ and I^- currents, have been represented in Fig. 3 as functions of the pore radius. Due to the doubling of the numbers of simulated trajectories for each ensemble, the achieved accuracy is significantly higher than for

the similar plots in Paper I. The comparatively larger error bars corresponding to CNT (10,10) (Fig. 3) are to be ascribed (according to the argumentation in Paper I) to the intermediate role assumed by this pore between the flow regimes with sporadic ion passages through the low-diameter pores and the "gating" regime specific to higher chiralities. In any case, these error estimates do not affect the essence of the slope discontinuities in the partial currents and of the following analysis. An important qualitative finding is that the average net current, while still affected by discrete fluctuation is significantly smoother than the partial currents, whose oscillations appear to be compensating each other in the total current. Moreover, instead of possibly reducing with doubled data collection time (0.8 μs), the discontinuities of the partial currents (indicated in Fig. 3 by the vertical arrow) become even more explicit. A very illustrative explanation of this behavior is provided by the mentioned theoretical works of Zwolak and co-workers.[8,9] Essentially, the model relies on the one-dimensional steady-state Nernst-Planck equation, expressing the charge flux for ion species ν as

$$J_\nu = -q_\nu D_\nu \left[\frac{dn_\nu}{dz} + \frac{q_\nu}{k_B T} n_\nu \frac{d\Phi_\nu}{dz} \right], \tag{2}$$

where q_ν is the charge, D_ν is the diffusion coefficient, n_ν is the number density, and Φ_ν is the axial potential. Several simplifying assumptions are reasonable. (1) The ion densities in the reservoirs are constant and equal to n_0 (satisfied on average in the simulations). (2) The electrostatic potential drops linearly over the pore, as $\Phi_\nu = zE_z + \Delta F_\nu / q_\nu$, where E_z is the constant electric field and ΔF_ν is the free energy change for a single ion between the bulk and the nanopore (satisfied to a good approximation as seen from the axial potential plots in Fig. 10 of Paper II). (3) The ionic density in the pore is small and thus the field inside the CNT results from the ionic charge layers at the membrane walls (satisfied according to the average axial density plots in Fig. 4 of Paper I). Finally, relating the diffusion coefficient to the mobility via the Einstein relation, $\mu_\nu = q_\nu D_\nu / k_B T$, one obtains for the charge flux

$$J_\nu = -q_\nu n_0 \mu_\nu E_z \exp(-\Delta F_\nu / k_B T). \tag{3}$$

Now, owing to the strong overall decrease of ΔF_ν with increasing pore radius, which is marked additionally by significant slope discontinuities corresponding to the cases where the effective (not the geometric) pore radius coincides with a hydration shell radius (see, for instance, Fig. 3 of Ref. 8), the above expression of the charge flux depends actually in a steplike, exponentially increasing manner on the effective pore radius.

For an axial electric field of 1 mV/Å (five times smaller than the smallest field considered in the present work), Zwolak *et al.*[9] predict a first current discontinuity for Na^+ and Cl^- corresponding to an effective pore radius around 5.1 and, respectively, 4.9 Å. For Na^+ we find, indeed, a discontinuity between two regions of exponential increase for the CNT (10,10) (radius 6.77 Å), pointed at in Fig. 3, as mentioned before, by a vertical arrow. Recalling that in Paper I we have defined the effective pore radius as $r_{\text{pore}}^{\text{eff}} = r_{\text{pore}} - \sigma_{\text{graph}}$, with $\sigma_{\text{graph}} = 1.674$ Å half the graphite inter-plane distance,

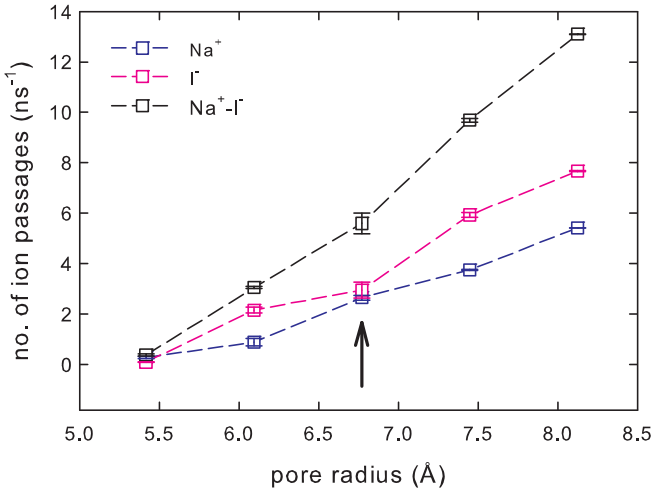

FIG. 3. Average total number of ion passages per nanosecond (upper plot) for a NaI solution comprising 30 ions and subject to an axial electric field of 0.02 V/Å as a function of the CNT radius. The discontinuity of the partial currents for Na^+ (lower plot) and I^- (middle plot) is indicated by the arrow.

we have for the CNT in question $r_{\text{pore}}^{\text{eff}} = 5.10$ Å, and thus an excellent agreement with the value predicted by the analytical model for Na^+. However, the discontinuities found in the present simulations are obviously less pronounced than those predicted by the theory of Zwolak *et al.*

To conclude this discussion, we need to stress that, inasmuch as the partial ionic currents are concerned, a quantization of the ionic conductance of the CNT manifests itself by step-wise current discontinuities separating regions of exponential increase with increasing nanopore radius. As for the net currents, their behavior is much smoother due to the clear tendency of the discontinuities of the partial currents to compensate each other. Moreover, the assertion of Zwolak *et al.*,[9] that the ion type plays merely a marginal role in this phenomenon, is not supported by our simulations, the discontinuous behavior for the NaCl solution being less distinct than the one for the NaI solution.

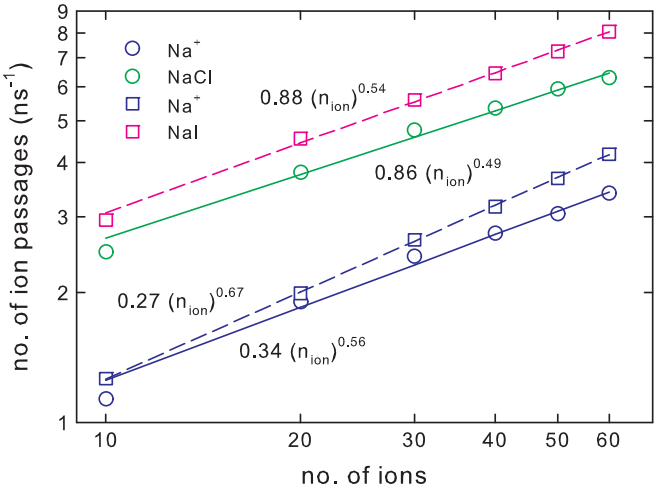

FIG. 4. Log-log plots of the average net numbers of ion passages per ns through the CNT (10,10), for NaCl and NaI solutions subject to an axial electric field of 0.02 V/Å, as functions of the ion concentration. The lower pair of dependences corresponds to the partial currents due to the Na^+ ions solely.

Figure 4 shows the net ionic currents through the CNT (10,10) filled with NaCl and NaI solutions, in the presence of an axial electric field of 0.02 V/Å, as functions of the total number of solvent ions. The particular log-log representation is actually meant to evidence the quasi-linearity of the plots, which, in turn, implies the proportionality between the logarithm of the nanochannel *conductance* and the logarithm of the solute *concentration*. This power-law behavior departs from the linear current-concentration dependence, one would expect for a homogeneous system due to the pronounced accumulation of ions in the radial density maxima with increasing concentration (upper panel of Fig. 1 of Paper II) and can be directly linked to the corresponding power-law dependence of the axial potential drop experienced by the transiting ions (lower panel of Fig. 11 of Paper II). This finding is perfectly consistent with the linear regime in the log-log plots of KCl concentration versus nanochannel conductance reported by Stein *et al.*[21] and by Schoch *et al.*[12] in the concentration range above 0.1M, where also the present concentrations are situated.

Similar to the ascending pore radius dependences presented in Paper I (Fig. 14), the present concentration dependences of the ionic currents (though saturating when plotted on regular linear scale) highlight the same ion specificity, which, in the particular case of the considered CNT, favors I^- compared to Cl^- increasingly, evolving steadily in the considered solute concentration range from 17% to 25%. The average difference in the partial Na^+ currents grows through lower values from only 11% to 21%. As pointed out in Paper I, the ion specificity can be linked directly to the qualitatively different radial density patterns inside the pore, with the I^- ions transiting the CNT on average along cylindrical layers of larger diameter.

The somewhat better linearity of the current profiles corresponding to the NaI solution (as seen in Fig. 4) is clearly another consequence of the simpler structure of the radial density profiles in the case of the I^- ions as compared to the Cl^- ions. Despite the apparently close slopes for each of the cation-anion pairs, there is, however, a moderate but steady increase of the weight of the partial Na^+ currents within the net currents with increasing solute concentration for both solute types. In the case of the NaCl solution, the increase from 10 to 60 solute ions is accompanied by a monotonic increase from 46% to 54% of the partial Na^+ current, while in the case of the NaI solution, the increase is from 43% to 52%.

The non-vanishing net water fluxes, illustrated by the concentration-dependent plots of Fig. 5, demonstrate that the solute ions transit the CNT surrounded by their solvation shells, reflecting, at the same time, the differing relative weights of the partial currents within the net ionic current. The increasingly predominant contribution of the Na^+ ions, discussed above, results in positive water fluxes (in the positive z-direction in which the electric field drives the Na^+ ions) for both solute types. The relatively small net number of water molecules driven by the solute ions does not allow one to qualitatively extrapolate the findings to higher solute concentrations, yet an incipient saturating evolution can be identified, especially in the NaI case.

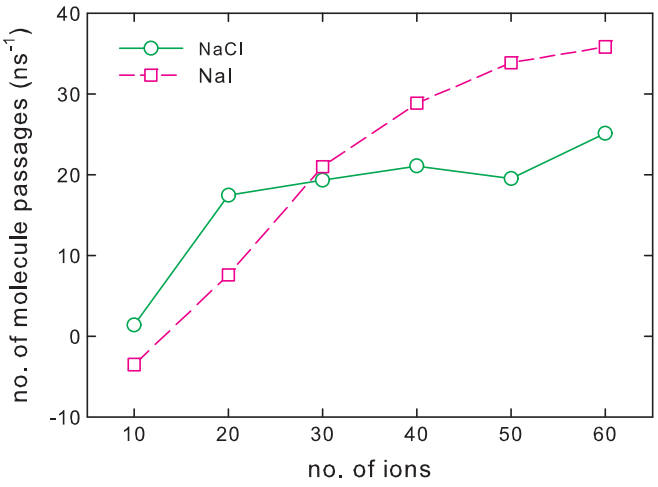

FIG. 5. Average net number of H_2O molecule passages per ns through the CNT (10,10) for NaCl and NaI solutions subject to an axial electric field of 0.02 V/Å as functions of the total number of ions.

The average ion passage times, plotted in Fig. 6 as functions of the total number of solute ions, represent, as defined in Paper I, average time intervals during which the ions executing *successful passages* reside effectively inside the pore. This definition differs from the average time in which the channel is simply populated by ions; since it excludes ions merely entering the pore and re-exiting to the same reservoir and, moreover, ions possibly not leaving the pore at all.

The ion passage times range for all ion species between 0.48 and 0.96 ns, showing a gradual increase with the solute concentration as the ion trajectories become more sinuous due to the reciprocal obstruction of identical ions and the cation-anion pairing phenomenon, which is discussed below. In particular, the passage time for the Cl^- ions can be seen to double for a sixfold increase in concentration. The corresponding drift velocities cover the interval 60–125 Å/ns.

The CNT selectivity, substantiated by the higher net currents for the NaI solute, can be now linked, besides the already invoked qualitatively different radial density distributions of

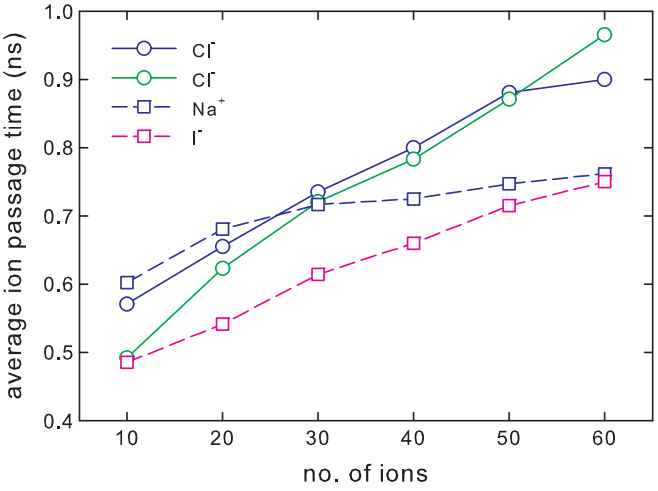

FIG. 6. Average passage times of the ions through the CNT (10,10) for NaCl and NaI solutions subject to an axial electric field of 0.02 V/Å as functions total number of ions.

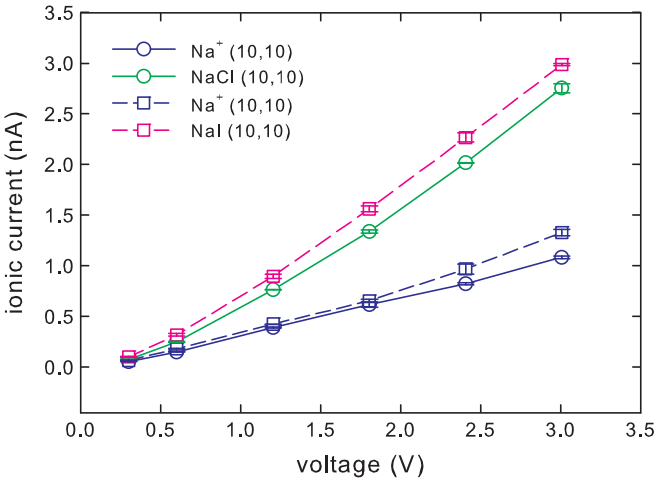

FIG. 7. Average ionic currents through a CNT (10,10) of length 60.17 Å for NaCl and NaI solutions composed of 30 solute ions as functions of the applied voltage. The lower pair of dependences corresponds to the partial currents due to the Na^+ ions solely.

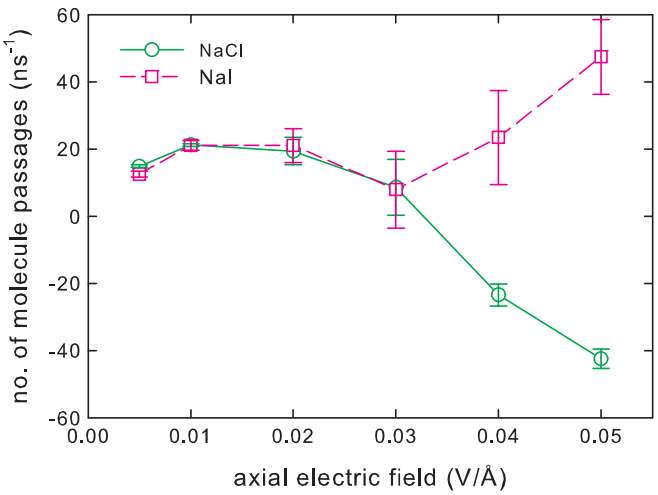

FIG. 8. Average net number of H_2O molecule passages per ns through the CNT (10,10) for NaCl and NaI solutions subject to an axial electric field of 0.02 V/Å as functions of the axial electric field.

the Cl^- and I^- anions, to the generally higher pore/reservoir density ratio of the NaI components (Fig. 3 of Paper II) and their generally lower passage times (Fig. 6).

As can be seen from Fig. 7, the ion currents show a marked, albeit not pronouncedly nonlinear dependence on the uniform electric field applied along the channel axis, which results in voltages between the ends of the 60.17 Å long CNT (10,10) of up to about 3 V. For a tenfold increase in the applied electric field (voltage) there is an increase of roughly 20 times in the partial Na^+ currents and of about 40, respectively, 30 times in the total net currents for the NaCl and NaI solutions.

The shape of the voltage-current curve can be explained on the basis of the charge flux given by Eq. (3), wherefrom, by invoking the linearly decaying dependence of the free energy change of the ions between the bulk and the nanopore center on the electric field, $\Delta F_\nu = q_\nu \left(\Phi_\nu - z_{\text{pore}} E_z\right)$, one obtains the qualitative behavior found in the simulations,

$$J_\nu \sim E_z \exp[q_\nu (z_{\text{pore}} E_z - \Phi_\nu)/k_{\text{B}}T], \tag{4}$$

at the same time vanishing for $E_z = 0$, behaving roughly linearly for low fields and growing exponentially for larger ones.

Like in the case of the pore radius dependences discussed in Paper I, the selectivity of the CNTs to the anion species is apparent also in the voltage-current curves, the total currents corresponding to the NaI solution exceeding on average by 18% the ones for the NaCl solution. This relies again on the fact that the I^- anions transit the CNTs preferentially via cylindrical layers of larger average radius which can hydrate a larger number of ions. The apparently proportional evolution for each of the cation-anion pairs actually conceals a moderate but steady decrease of the weight of the partial Na^+ currents within the net currents with increasing electric field. In the case of the NaCl solution, the tenfold increase in the voltage between the ends of the CNT (from 0.03 to 0.3 V) roughly results in the halving of the partial Na^+ current (from 73% to 39%), while in the case of the NaI solution, the decrease is less pronounced (from 65% to 44%).

Somewhat surprising, though insightful and deserving closer attention, are the net water fluxes through the CNT as functions of the applied axial electric field (Fig. 8). The reason for interest is, evidently, the discontinuities featured by the dependences for both solute types, which separate an *anion non-specific* from an *anion-specific* regime.

Up to the critical electric field strength of 0.03 V/Å, the water fluxes, amounting to less than 20 molecules per ns, appear to be spurious, since they are of the order of magnitude of the net ion currents. In particular, for 0.03 V/Å, the net number of passages per ns equal ≈ 8.3 for the water molecules, ≈ 8.4 for the NaCl components, and ≈ 9.7 for the NaI components. However, the almost perfect overlap of the net water fluxes for the NaCl and NaI solutions rules out the possibility of numerical artifacts, while their low values indicate an almost perfect balance between the partial currents of cations and anions. Even though the CNT does not distinguish between different anion species, the cation-anion separation proceeds optimally in this domain, producing a minimal water flux.

The interesting point is that beyond 0.03 V/Å, the profiles for the two solute types start abruptly evolving in opposite directions, almost symmetrically. The positive water fluxes in the case of the NaI solution suggest a Na^+ (cation) dominated current, while the negative values in the case of the NaCl solution correspond to a Cl^- (anion) dominated current in opposite direction to the electric field. Evidently, both cases give rise to positive equivalent charge flows. This qualitative behavior difference is in line with the more substantial decrease of the weight of the partial Na^+ currents for the NaCl solution, which was mentioned before.

From a structural perspective, the anion-specific behavior reflected in the net water fluxes can be linked to the overhydration of around 5% of the Cl^- ions with respect to I^-, which was found in Paper II to be approximately conserved for all considered axial electric fields. The higher Cl–H coordinations clearly involve a larger number of water molecules being driven along the CNT as hydration shells, thus leading

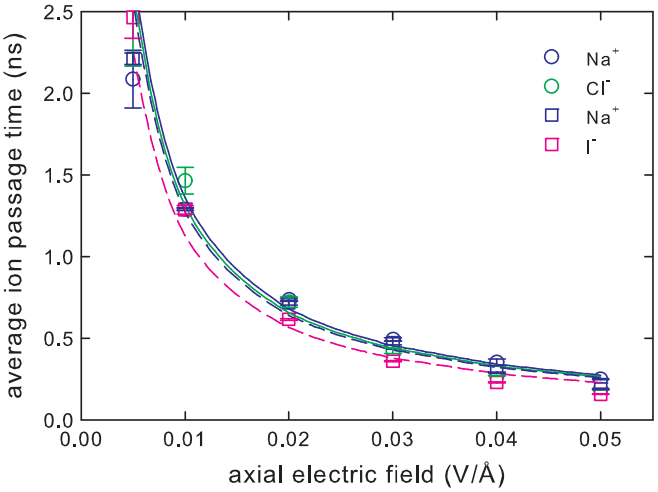

FIG. 9. Average passage times of the ions through the CNT (10,10) for NaCl and NaI solutions composed of 30 solute ions as functions of the axial electric field. Continuous lines represent the hyperbolic fits for the NaCl solution and dashed lines, those for the NaI solution.

to larger partial anion currents and, consequently, to the reversed (negative) water fluxes accompanying the Cl^- ions.

The average ion passage times, plotted in Fig. 9 as functions of the applied axial electric field, can be fairly well fitted with hyperbolic decays reflecting the proportionality between the average drift velocity of the transiting ions and the applied electric field ($v_z = \mu_z E_z$). Even if the profiles for all ion species appear to be well grouped, the relative ordering with the I^- ions having the shortest translocation times, found also in the case of the pore radius and solute concentration dependences, holds here again.

The drift velocities corresponding to the passage times discussed above cover the interval 0.02–0.38 Å/ps. As the applied electric fields themselves, the drift velocities for Na^+ are roughly one order of magnitude lower than the values reported by Dzubiella *et al.* (0.4–2.3 Å/ps).[3] Furthermore, while the present drift velocities maintain to a fair extent the proportionality to the electric field throughout the considered range (0.005–0.05 V/Å), those of Ref. 4 appear to be depending nonlinearly on the average internal electric field (0.11\break–0.32 V/Å).

The average drift mobilities can be estimated straightforwardly from the average passage times t_z as $\mu_z = L^{\text{eff}}_{\text{pore}}/t_z E_z$, where the effective nanopore length was defined in Paper I in terms of the geometric half-length by $L^{\text{eff}}_{\text{pore}} = 2(z_{\text{pore}} + \sigma_{\text{graph}}) = 63.52$ Å. The drift mobilities for the translocations through the CNT (10,10) are listed in Table I along with the mobilities derived from the diffusion coefficients presented in Sec. III A ($\mu_D = qD/k_B T$). An immediate finding, confirming the consistency of their definitions, concerns the generally lower values of the drift velocities ($\mu_z \lesssim \mu_D$), which account only for the directional motion along the nanochannel axis. From this perspective and the comparatively larger increase of the diffusional mobilities (with up to a factor of 2), one can conclude that, indirectly, by means of the structural changes they cause, the electric fields enhance to a significant extent also the motion perpendicular to the channel axis. In addition, the higher average mobility of the I^- anions, consequence of their privileged, outer average radial positions in the CNTs, emerges anew. More than from the diffusional mobilities, the anion specificity is visible from the drift mobilities, which are on average about 17% higher for I^- than for Cl^-.

TABLE I. Mobilities (in $Å^2$/V ps) for the ions of the NaCl and NaI solutions inside the CNT (10,10), μ_z (derived from the average passage times) and μ_D (derived from the diffusion coefficients) for different axial electric fields (in V/Å). The values in the penultimate row correspond to the hyperbolic fits of Fig. 9 and the experimental bulk values are from Ref. 22.

	Na^+		Cl^-		Na^+		I^-	
E_z	μ_z	μ_D	μ_z	μ_D	μ_z	μ_D	μ_z	μ_D
0.01	4.66	5.17	4.11	5.59	4.67	4.58	4.68	5.60
0.02	4.09	5.31	4.18	5.28	4.20	4.90	4.90	6.18
0.03	4.08	6.14	4.75	6.60	4.26	5.81	5.60	7.23
0.04	4.27	7.69	5.57	8.99	5.18	8.81	6.54	9.08
0.05	4.83	10.17	6.48	12.77	6.37	12.02	7.67	12.00
Fit	4.67		4.84		4.97		5.63	
Bulk (Ref. 22)	5.17		7.91		5.17		7.97	

With a view to characterize the transport process by means of single-valued mobilities, independent of the applied voltage, these can be derived from the hyperbolic fits of the ion passage times with respect to the axial electric field ($t_z = L^{\text{eff}}_{\text{pore}}/\mu_z E_z$). The obtained values (listed in Table I in the row labeled "fit"), are essentially close (within less than 3%) to the average of the field-dependent mobilities. In the considered range of electric field strengths, the drift mobilities μ_z can be seen to be generally limited by the bulk values reported by Lee *et al.*[22] and, in any case, the fitted mobilities are without exception inferior. An interesting aspect is that, while in the bulk the anion mobilities exceed by up to 35% those of Na^+, in the CNTs this difference is reduced to less than 12%. A contribution to the leveling of the cation and anion mobilities can be attributed to the ion pairing effect, which is susceptible of impeding the opposite drifts of the cation and ion due to the implied Coulomb attraction.

C. Ion pairing

The correlated motion of cation-anion pairs in solutions can be described by the concept of ion pairing, which was developed by Bjerrum[23] and is central to stereochemistry. The concept was employed by Nicholson and Quirke[24] in equilibrium simulations of NaCl solutions confined in cylindrical spaces, as part of an analysis based on radial distribution functions (RDFs). The studies of Fennell *et al.*[25] deal with the ion pairing effect in bulk solutions and characterize it by the potential of mean force, whereas Palmeri *et al.*[26] describe the phenomenon by time correlation functions, which are restricted, however, to nearest neighbors as provided by the RDFs.

As a quantitative measure of ion pairing, differing from those reported so far, but being at the same time general and yet better adapted to the particular geometry of the system, we have employed the *relative ion pairing time*, de-

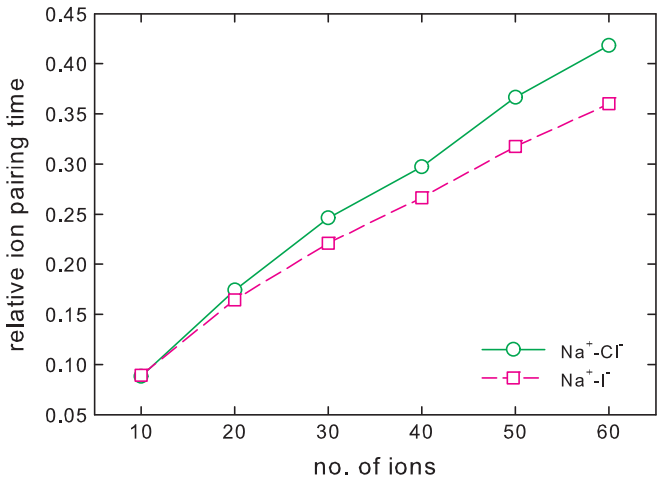

FIG. 10. Relative ion pairing times in the CNT (10,10) for NaCl and NaI solutions subject to an axial electric field of 0.02 V/Å as functions of the solute ion concentration.

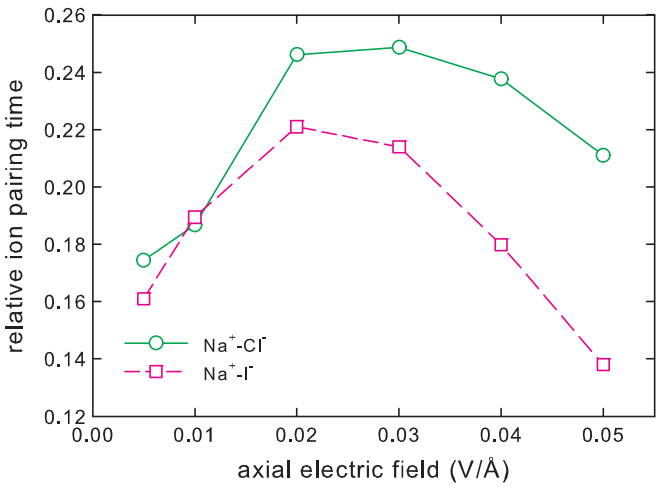

FIG. 11. Relative ion pairing times in the CNT (10,10) for NaCl and NaI solutions composed of 30 solute ions as functions of the axial electric field.

fined as the ratio between the cumulated time in which the cation-anion pairs situated at axial distances smaller than 10 Å have same-sign z-velocity components and the cumulated residence time of the ions inside the nanotube. The alternative definition using the *relative distance* the cation-anion pairs travel correlated inside the CNT provides similar findings. Due to the high anisotropy of the system, the cutoff was chosen somewhat larger than the so-called Bjerrum length, $\lambda_B = e^2/4\pi\varepsilon_0\varepsilon_r k_B T$ (the separation at which the electrostatic interactions are comparable to the thermal energy scale),[27] which amounts at 300 K to ~7 Å for water.

The ion pairing times grow monotonically with increasing pore radius, without relevant anion specificity and reaching a relative value of about 0.33 for the widest pore considered, i.e., the CNT (12,12). The profiles of the ion pairing times depending on the solute concentration (Fig. 10) are slightly nonlinear, vanishing alike for both solute types in the low-concentration region and showing an emerging saturation tendency for higher concentrations. The ion specificity of the CNT interior manifests itself by the longer relative correlation times for Na^+–Cl^- than for Na^+–I^- and the difference grows more pronounced the higher the solute concentration becomes. On the other hand, this finding is consistent with the lower ionic currents found throughout for the NaCl solution.

Being non-monotonic, the most inciting dependences of the ion pairing times are the ones on the axial electric field (Fig. 11). At low field strengths they are ascending, while for larger fields they decrease monotonically. Again, like in the case of the water fluxes driven through the nanotube by the ionic currents, the electric field interval around 0.02 –0.03 V/Å (otherwise typical for biophysical nanosystems) acts as separation between domains of qualitatively different behavior. The increase of the correlation times actually accompanies the rise of the pore/reservoir density ratios induced by the increasing voltage (according to Fig. 5 of Paper II), which thus indirectly enhances the probability of cation-anion pairs reaching within the correlation cutoff with modest same-sign z-components of the velocities. However, the further increase of the applied field, beyond 0.03 V/Å, does not produce a further increase of the relative ion population inside the pore and the accompanying increase of the relative drift velocities, combined with the transition to the "gating" regime characterized by alternating, increasingly intense cascades of either cations or anions, actually tends to depopulate the pore and to render pairing less probable.

The ion specificity of the CNTs is in line with the consistently higher ionic currents and the lower ion pairing for the NaI solution as compared to the NaCl solution, the ion pairing phenomenon turning out to have a diminishing effect on the ionic currents.

IV. CONCLUSIONS

This third paper in a series dedicated to the systematic MD study of the ion transport through "armchair"-type (n, n) CNTs filled with NaCl and NaI solutions focuses primarily on the effects the solute concentration and axial electric fields produce on the transport properties. Correlations between the structural properties (presented in Paper II) and the dynamic properties have been established, linking causally the radial density profiles and the ion pairing phenomenon with the ionic currents and charge carrier mobilities. Due to the large data collection times cumulated for each trajectory ensemble (0.8 μs), significantly larger than the ones previously reported in the literature, the findings of this work can be useful both as tests of general theoretical nanofluidics results and as counterparts for experimental measurements.

The diffusion coefficients inside the CNT have been found to decrease slightly nonlinearly with increasing solute concentration, similar to the experimental and theoretical behavior reported by Turq and co-workers.[19,20] The reduced diffusion in the pores is determined by the constrained average flow along cylindrical flux layers and by the fact that the ions travel partially surrounded by their solvation shells.

Complementing the results of Paper I and contrary to the rather smooth behavior found for the *net* ionic currents, step-wise discontinuities of the *partial* ionic currents,

separating regions of roughly exponential increase with increasing nanopore radius, have been evidenced. The discontinuous behavior supports the model of quantized ionic conductance in nanopores developed recently by Zwolak and co-workers[8,9] and, for Na^+, the agreement between the predicted and simulated *effective* pore radius corresponding to the first discontinuity is remarkable (5.1 Å). This finding reflects the resonant effect of the complete stripping of the hydration shell (caused by the coincidence of the effective pore radius with the hydration shell radius) on the free energy change the ions experience between reservoir and the nanopore interior.

A power-law (linear log-log) dependence on the solute concentration has been identified for the CNT conductance and this general nanofluidic result is similar to the linear regime described in the literature.[12,21] The voltage-current curves are markedly ascending, though not pronouncedly nonlinear for both solute types. Analytically, this behavior results from the applied electric field entering both linearly and exponentially the expression of the charge flux through the CNT. The intrinsic anion specificity of the CNTs favors I^- as compared to Cl^- typically by about 20% both in the concentration-current and the voltage-current curves.

The average ion passage times decay roughly hyperbolically with increasing applied voltage, reflecting the approximate proportionality of the average drift velocity of the ions with the axial electric field. The mobilities determined from the diffusion coefficients are consistently larger than the drift mobilities derived from the passage times and, at the same time, more sensitive to the electric field, which appears to enhance also the transverse ion mobility. A specific effect, that can be identified also in the case of ion pairing, is the significant leveling (reduction of the relative difference) of the drift mobilities of cations and anions within the pore as compared to the bulk phase.

A new quantitative measure for ion pairing is proposed, i.e., the relative ion pairing time, defined as the ratio of the cumulated time in which the cation-anion pairs move correlated and their total residence time inside the pore. The ion pairing times grow steadily with increasing pore radius and/or solute concentration. The concentration dependences, in particular, show an increasingly anion-specific behavior inside the CNT by longer relative correlation times for the Na^+–Cl^- as compared to the Na^+–I^- pairs. The non-monotonic dependences of the pairing times on the axial electric field evidence clearly anion specificity and reveal two flow regimes at electric field strengths of biological relevance. Up to about 0.03 V/Å, the main effect is the increase of the ion population within the pore, which makes more probable cation-anion encounters at moderate distances and low velocities with same-sign z-components. The further increase of the applied electric field, however, leads to a saturation of the pore/reservoir density ratios and reduces the ion pairing due to the increasing cation-anion relative drift velocity and the cascading ion passages.

ACKNOWLEDGMENTS

This work was supported by CNCSIS-UEFISCSU, project number PNII-ID PCCE_129/2008.

[1] T. A. Beu, J. Chem. Phys. **132**, 164513 (2010).
[2] T. A. Beu, J. Chem. Phys. **135**, 044515 (2011).
[3] J. Dzubiella, R. J. Allen, and J.-P. Hansen, J. Chem. Phys. **120**, 5001 (2004).
[4] J. Dzubiella and J.-P. Hansen, J. Chem. Phys. **122**, 234706 (2005).
[5] C. Peter and G. Hummer, Biophys. J. **89**, 2222 (2005).
[6] B. Corry, J. Phys. Chem. B **112**, 1427 (2008).
[7] C. Song and B. Corry, J. Phys. Chem. B **113**, 7642 (2009).
[8] M. Zwolak, J. Lagerqvist, and M. Di Ventra, Phys. Rev. Lett. **103**, 128102 (2009).
[9] M. Zwolak, J. Wilson, and M. Di Ventra, J. Phys.: Condens. Matter **22**, 454126 (2010).
[10] F. G. Donnan, Chem. Rev. **1**, 73 (1924).
[11] F. G. Donnan, J. Membr. Sci. **100**, 45 (1995).
[12] R. B. Schoch, J. Han, and P. Renaud, Rev. Mod. Phys. **80**, 839 (2008).
[13] D. C. Rapaport, *The Art of Molecular Dynamics Simulation* (Cambridge University Press, Cambridge, England, 1995).
[14] R. W. Hockney and J. W. Eastwood, *Computer Simulation Using Particles* (IOP, Bristol, 1988).
[15] M. Deserno and C. Holm, J. Chem. Phys. **109**, 7678 (1998); *ibid*., **109**, 7694 (1998).
[16] W. L. Jorgensen, J. Chandrasekhar, J. D. Madura, R. W. Impey, and M. L. Klein, J. Chem. Phys. **79**, 926 (1983).
[17] M. W. Mahoney and W. L. Jorgensen, J. Chem. Phys. **112**, 8910 (2000).
[18] J. M. Xue, X. Q. Zou, Y. B. Xie, and Y. G. Wang, J. Phys. D: Appl. Phys. **42**, 105308 (2009).
[19] J.-F. Dufrêche, A.-L. Rollet, M. Jardat, and P. Turq, J. Mol. Liq. **96**, 113 (2002).
[20] J.-F. Dufrêche, O. Bernard, and P. Turq, J. Mol. Liq. **118**, 189 (2005).
[21] D. Stein, M. Kruithof, and C. Dekker, Phys. Rev. Lett. **93**, 035901 (2004).
[22] S. H. Lee and J. C. Rasaiah, J. Phys. Chem. **100**, 1420 (1996).
[23] N. K. Bjerrum, K. Dan. Vidensk. Selsk. Mat. Fys. Medd. **7**(1) (1926).
[24] D. Nicholson and N. Quirke, Mol. Simul. **29**, 287 (2003).
[25] C. J. Fennell, A. Bizjak, V. Vlachy, and K. A. Dill, J. Phys. Chem. B **113**, 6782 (2009).
[26] P.-A. Cazade, J. Dweik, B. Coasne, F. Henn, and J. Palmeri, J. Phys. Chem. C **114**, 12245 (2010).
[27] W. B. Russel, D. A. Saville, and W. R. Schowalter, *Colloidal Dispersions* (Cambridge University Press, New York, 1989).